
Copulas as High-Dimensional Generative Models: Vine Copula Autoencoders

Natasa Tagasovska
Department of Information Systems
HEC Lausanne
Switzerland
natasa.tagasovska@unil.ch

Damien Ackerer
Swissquote Bank
Gland, Switzerland
damien.ackerer@swissquote.ch

Thibault Vatter
Department of Statistics
Columbia University
New York, USA
thibault.vatter@columbia.edu

Abstract

We propose a vine copula autoencoder to construct flexible generative models for high-dimensional distributions in a straightforward three-step procedure. First, an autoencoder compresses the data using a lower dimensional representation. Second, the multivariate distribution of the encoded data is estimated with vine copulas. Third, a generative model is obtained by combining the estimated distribution with the decoder part of the autoencoder. This approach can transform any already trained autoencoder into a flexible generative model at a low computational cost. This is an advantage over existing generative models such as adversarial networks and variational autoencoders which can be difficult to train and can impose strong assumptions on the latent space. Experiments on MNIST, Street View House Numbers and Large-Scale CelebFaces Attributes datasets show that vine copulas autoencoders can achieve competitive results to standard baselines.

1 Introduction

Exploiting the statistical structure of high-dimensional distributions behind audio, images, or video data is at the core of machine learning. Generative models aim not only at creating feature representations, but also at providing means of sampling new realistic data points. Two classes are typically distinguished: *explicit* and *implicit* generative models. Explicit generative models make distributional assumptions on the data generative process. For example, *variational autoencoders* (VAEs) assume that the latent features are independent and normally distributed [35]. Implicit generative models make no statistical assumption but leverage another mechanism to transform noise into realistic data. For example, *generative adversarial networks* (GANs) use a discriminant model penalizing the loss function of a generative model producing unrealistic data [20]. Interestingly, *adversarial autoencoders* (AAEs) combined both features as they use a discriminant model penalizing the loss function of an encoder when the encoded data distribution differs from the prior (Gaussian) distribution [46]. All of these new types of generative models have achieved unprecedented results and also proved to be computationally more efficient than the first generation of deep generative models required Markov chain Monte Carlo methods [30, 28]. However, adversarial approaches require multiple models to be trained, leading to difficulties and computational burden [58, 24, 22], and variational approaches make strong distributional assumptions, potentially detrimental to the generative model performance [59].

Preprint. Under review.

We present a novel approach to construct a generative model which is simple, makes no prior distributional assumption, and is computationally efficient: the *vine copulas autoencoders* (VCAEs). Our approach, schematized in Figure 1 combines three tasks. First, an autoencoder is trained to compress the data into a lower dimensional space. Second, the multivariate distribution of the encoded data is estimated with vine copula, namely, flexible tool to construct high-dimensional multivariate distributions [3, 4, 1]. Third, a generative model is obtained by combining the estimated vine copula distribution with the decoder part of the autoencoder.

In other words, new data is produced by decoding random samples generated from the vine copula. An already trained autoencoder can thus be transformed into a generative model, where the only additional cost would be the estimation of the vine copula. We show in multiple experiments that this approach performs well in building generative models for the MNIST, Large-Scale CelebFaces Attributes, and Street View House Numbers datasets. To the best of our knowledge, this is the first time that vine copulas are used to construct generative models for very high dimensional data (such as images).

Next, we review the related work most relevant to our setting. The most widespread generative models nowadays focus on synthetic image generation, and mainly fall into the GAN or VAE categories, some interesting recent developments include [47, 13, 24, 70, 27]. These modern approaches have been largely inspired by previous generative models such as belief networks [30], independent component analysis [31] or denoising autoencoders [73]. Part of their success can be attributed to the powerful neural network architectures which provide high quality feature representations, often using Convolutional architectures [39]. A completely different framework to model multivariate dependencies has been developed in the statistical literature: the so-called *copulas*. Thanks to their ability to capture complex dependence structures, copulas have been applied to a wide range of scientific problems, and their successes have led to continual advances in both theory and open-source software availability. We refer to [53, 33] for textbooks introductions. More recently, copulas also made their way into machine learning research [41, 18, 45, 72, 43, 12]. However, such approaches have not leveraged their usefulness as generative models. While [40, 56] use copulas for synthetic data generation, they rely on strong parametric assumptions. In this work, we illustrate how *nonparametric vine copulas* allow for arbitrary density estimation [48], which in turn can be used to sample realistic synthetic datasets.

Because their training is relatively straightforward, VCAEs have some advantages over GANs. For instance, GANs require improved (i.e., more complex) versions of the vanilla algorithm to avoid mode collapse, whereas vines naturally fit multimodal data. Additionally, while GANs suffer from the “exploding gradients” phenomenon (e.g., see [22]) and require careful monitoring of the training and early stopping, this is not an issue with VCAEs.

It should also be noted that a VCAE turns any AE into a generative model. As such, the AE can be used and fine-tuned to simultaneously achieve other purposes (e.g., denoising, clustering), whereas a GAN arguably has a single purpose.

The remainder of the paper is as follows. Section 2 reviews vine copulas as well as their estimation and simulation algorithms. Section 3 discusses the vine copula autoencoder approach. Section 4 presents the results of our experiments. Section 5 concludes and discusses future research. The supplementary material contains further information on algorithm and experiments, as well as additional experiments.

2 Vine copulas

2.1 Preliminaries and motivation

A copula, from the latin word *link*, flexibly “couples” marginal distributions into a joint distribution. As such, copulas allow to construct joint distributions with the same margins but different dependence structures, or conversely by fixing the dependence structure and changing the individual behaviors.

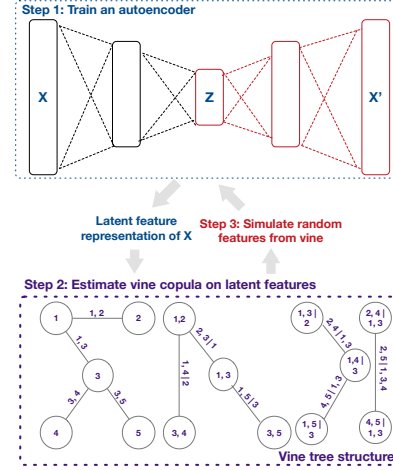


Figure 1: Vine Copula Autoencoder.

Thanks to this versatility, there has been an exponentially increasing interest in copula-based models over the last two decades. One important reason lies in the following theorem.

Theorem 1 (Sklar’s theorem [66]). *The continuous random vector $\mathbf{X} = (X_1, \dots, X_d)$ has joint distribution F and marginal distributions F_1, \dots, F_d if and only if there exist a unique copula¹ C , which is the joint distribution of $\mathbf{U} = (U_1, \dots, U_d) = (F_1(X_1), \dots, F_d(X_d))$.*

Assuming that all densities exist, we can write $f(x_1, \dots, x_d) = c\{u_1, \dots, u_d\} \times \prod_{k=1}^d f_k(x_k)$, where $u_i = F_i(x_i)$ and f, c, f_1, \dots, f_d are the densities corresponding to F, C, F_1, \dots, F_d respectively. As such, copulas allow to decompose a joint density into a product between the marginal densities and the dependence structure represented by the copula density.

This has an important implication for the estimation and sampling of copula-based marginal distributions: algorithms can generally be built into two steps. For instance, estimation is often done by estimating the marginal distributions first, and then using the estimated distributions to construct pseudo-observations via the probability integral transform before estimating the copula density. Similarly, synthetic samples can be obtained by sampling from the copula density first, and then using the inverse probability integral transform to transform back the copula sample to the natural scale of the data. We give a detailed visual example of both the estimation and sampling of (bivariate) copula-based distributions in Appendix A.2.

The availability of higher-dimensional models is rather limited, yet there exists numerous parametric families in the bivariate case. This has inspired the development of hierarchical models, constructed from cascades of simpler building blocks. Thanks to its flexibility and computational efficiency, the *pair-copula construction* (PCC), a new class of simple yet versatile models, has quickly become the most promising of such hierarchical structures and a hot-topic of multivariate analysis [2].

2.2 Vine copulas construction

Popularized in [3, 4, 1], PCCs model the joint distribution of a random vector by *decomposing the problem into modeling pairs of conditional random variables*, making the construction of complex dependencies both flexible and yet tractable. Let us exemplify such constructions using a three dimensional vector of continuously distributed random variables $\mathbf{X} = (X_1, X_2, X_3)$. The joint density f of \mathbf{X} can be decomposed as

$$f = f_1 f_2 f_3 c_{1,2} c_{2,3} c_{1,3|2}, \quad (1)$$

where we omitted the arguments for the sake of clarity, and f_1, f_2, f_3 are the marginal densities of X_1, X_2, X_3 , $c_{1,2}$ and $c_{2,3}$ are the joint densities of $(F_1(X_1), F_2(X_2))$ and $(F_2(X_2), F_3(X_3))$, $c_{1,3|2}$ is the joint density of $(F_{1|2}(X_1|X_2), F_{3|2}(X_3|X_2))|X_2$.

The above decomposition can be generalized to an arbitrary dimension d and leads to tractable and flexible probabilistic models [32, 3, 4]. While a decomposition is not unique, it can be organized as a graphical model called *regular vine*, *R-vine*, or simply *vine*, namely a sequence of $d-1$ trees. Denoting $T_m = (V_m, E_m)$ with V_m and E_m the set of nodes and edges of tree m for $m = 1, \dots, d-1$, the sequence is a vine if it satisfies a set of conditions guaranteeing that the decomposition leads to a *valid joint density*. The corresponding tree sequence is then called the *structure* of the PCC and has important implications to design efficient algorithms for the estimation and sampling of such models (see Section 2.3 and Section 2.4).

Each edge e is associated to a bivariate copula $c_{j_e, k_e | D_e}$ (a so-called *pair-copula*), with the set $D_e \in \{1, \dots, d\}$ and the indices $j_e, k_e \in \{1, \dots, d\}$ forming respectively its *conditioning set* and the *conditioned set*. Finally, the joint copula density can be written as the product of all pair-copula densities $c = \prod_{m=1}^{d-1} \prod_{e \in E_m} c_{j_e, k_e | D_e}$. In the following two sections, we discuss two topics that are important for the application of vines as generative models: estimation and simulation. For further details, we refer to the numerous books and surveys written about them [14, 37, 67, 16, 2].

2.3 Sequential estimation

To estimate vine copulas, it is common to follow a sequential approach [1, 25, 48], which we outline below. Assuming that the vine structure is known, the pair-copulas of the first tree, T_1 , can be directly estimated from the data. But this is not as straightforward for the other trees, since data from

¹A copula is a distribution function with uniform margins.

the densities $c_{j_e, d_e | D_e}$ are not observed. However, it is possible to sequentially construct “pseudo-observations” using appropriate data transformations, leading to the following estimation procedure, starting with tree T_1 : for each edge in the tree, estimate all pairs, construct pseudo-observations for the next tree, and iterate. The fact that the tree sequence T_1, T_2, \dots, T_{d-1} is a regular vine guarantees that at any step in this procedure, all required pseudo-observations are available. We further refer to [1, 11, 16, 17, 8, 34] for model selection methods and to [15, 68, 10, 25, 64] for more details on the inference and computational challenges related to PCCs. Importantly, vines can be truncated after a given number of trees [11, 7, 9] by setting pair-copulas in further trees to independence.

2.4 Simulation

Additionally to their flexibility, vines are easy to sample from using inverse transform sampling. Let C be a copula and $U = (U_1, \dots, U_d)$ is a vector of independent $U(0, 1)$ random variables. Then, define $V = (V_1, \dots, V_d)$ through $V_1 = C^{-1}(U_1)$, $V_2 = C^{-1}(U_2 | U_1)$, and so on until $V_d = C^{-1}(U_d | U_1, \dots, U_{d-1})$, with $C(v_k | v_1, \dots, v_{k-1})$ is the conditional distribution of V_k given V_1, \dots, V_{k-1} , $k = 2, \dots, d$. In other words, V is the inverse Rosenblatt transform [60] of U . It is then straightforward to notice that $V \sim C$, which can be used to simulate from C . As for the sequential estimation procedure, the fact that the tree sequence T_1, T_2, \dots, T_{d-1} is a regular vine guarantees that all required conditional bivariate copulas are available to compute the inverse Rosenblatt transform (see Algorithm 2.2 of [17]). Furthermore, there exist analytical expressions or good numerical approximations of such inverses for common parametric copula families. We refer to Section 2.5 for a discussion of the inverse computations for nonparametric estimators. The sampling algorithm for each pair copula constructs is given in Figure 2.

2.5 Implementation

To avoid specifying the marginal distributions, we use the Gaussian kernel density estimator with a bandwidth chosen using the direct plug-in methodology of [65].

Regarding the copula families used as building blocks for the vine, one can contrast parametric and nonparametric approaches. As is common in machine learning and statistics, the default choice is the Gaussian copula. In Section 2.6, we show empirically why this assumption (allowing for dependence between the variables but still in the Gaussian setting) can be too simplistic, resulting in failure to deliver even for three dimensional datasets.

Alternatively, using a nonparametric bivariate copula estimator provides the required flexibility. However, the bivariate Gaussian kernel estimator, targeted at densities of unbounded support, cannot be directly applied to pair-copulas, which are supported in the unit square. To get around this issue, the trick is to transform the data to standard normal margins before using a bivariate Gaussian kernel. Bivariate copulas are thus estimated nonparametrically using the transformation estimator [62, 45, 48, 19] defined as

$$\widehat{c}(u, v) = \frac{1}{n} \sum_{j=1}^n \frac{\mathcal{N}_{(\Phi^{-1}(u_j), \Phi^{-1}(v_j)), \Sigma}(\Phi^{-1}(u), \Phi^{-1}(v))}{\phi(\Phi^{-1}(u)) \phi(\Phi^{-1}(v))}, \quad (2)$$

with plug-in $\Sigma = n^{-1/3} \text{Cor}(\Phi^{-1}(U), \Phi^{-1}(V))$.

Along with vines-related functions (i.e., for sequential estimation and simulation), the Gaussian copula and (2) are implemented in C++ as part of `vinecopulib` [49], a header-only C++ library for copula models based on Eigen [23] and Boost [63]. In the following experiments, we use the R interface [57] interface to `vinecopulib` called `rvinecopulib` [51], which also include `kde1d` [50] for univariate density estimation.

Note that inverses of partial derivatives of the copula distribution corresponding to (2) are required to sample from a vine, as described in Section 2.4. Internally, `vinecopulib` constructs and stores a grid over $[0, 1]^2$ along with the evaluated density at the grid points. Then, bilinear interpolation

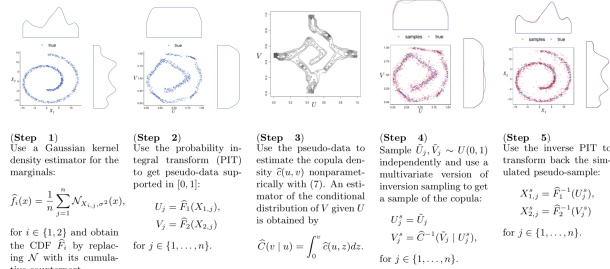


Figure 2: Sampling algorithm for a pair copula.

is used to efficiently compute the copula distribution $\hat{C}(u, v)$ and its partial derivatives. Finally, `vinecopulib` computes the inverses by numerically inverting the bilinearly interpolated quantities using a vectorized version of the bisection method.

2.6 Vines as generative models

To exemplify the use of vines as generative models, let us consider as a running example a three dimensional dataset X_1, X_2, X_3 with $X_1, X_2 \sim U[-5, 5]$ and $X_3 = \sqrt{X_1^2 + X_2^2} + U[-0.1, 0.1]$. The joint density can be decomposed as in the right-hand side of (1), and estimated following the procedures described in Section 2.5 and Section 2.3. With the structure and the estimated pair copulas, we can then use vines as generative models.

In Figure 3, we showcase three models. C1 is a nonparametric vine truncated after the first tree. In other words, it sets $c_{1,2|3}$ to independence. C2 is a nonparametric vine with two trees. C3 is a Gaussian vine with two trees. On the left panel, we show their vine structure, namely the trees and the pair copulas. On the right panel, we present synthetic samples from each of the models in blue, with the green data points corresponding to $\sqrt{X_1^2 + X_2^2}$.

Comparing C1 to C2 allows to understand the truncation effect: C2, being more flexible (fitting richer/deeper model), captures better the features of the joint distribution. It can be deduced from the fact that data generated by C2 looks like uniformly spread around the $\sqrt{X_1^2 + X_2^2}$ surface, while data generated by C1 is spread all around. It should be noted that, in both cases, the nonparametric estimator captures the fact that X_1 and X_2 are independent, as can be seen from the contour densities on the left panel. Regarding C3, it seems clear that Gaussian copulas are not suited to handle this kind of dependencies: for such nonlinearities, the estimated correlations are (close to) zero, as can be seen from the contour densities on the left panel.

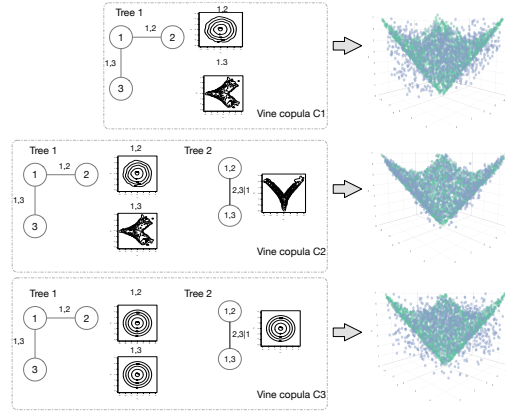


Figure 3: Simulating with different vine models.

With this motivation, the next section is dedicated to extending the vine generative approach to high dimensional data. While vines are theoretically suitable for fitting and sampling in high dimensions, they have been only applied to model a few thousands of variables. The reason is mainly that state-of-the-art implementations were geared towards applications such as climate science and financial risk computations. While software such as `vinecopulib` satisfies the requirements of such problems, even low-resolution images (e.g., $64 \times 64 \times 3$) are beyond its current capabilities. To address this challenge, we can rely on the embedded representations provided by neural networks.

3 Vine autoencoders

The other building block of the vine copula autoencoder is an *autoencoder* [6, 29]. These neural network models typically consist of two parts: an *encoder* f mapping a datum X from the original space \mathcal{X} to the latent space \mathcal{Y} , and a decoder g mapping a latent code Y from the latent space \mathcal{Y} to the original space \mathcal{X} . The autoencoder is trained to reconstruct the original input with minimal loss, that is $X' \approx g(f(X))$.

When f and g are linear and the loss is quadratic, the optimal solution is equivalent to principal component analysis with the same dimension as \mathcal{Y} . But more flexibility is obtained by letting f and g be nonlinear. To explore such complex classes of mappings, it is common to model the encoder and the decoder using neural network. Such deep autoencoders have been widely exploited in generative models because of their ability to transform high dimensional input spaces into relatively simple and low dimensional latent spaces.

However, autoencoders simply learn the most informative features to minimize the reconstruction loss, and therefore cannot be considered as generative models. In other words, since they do not learn the distributional properties of the latent features [5], they cannot be used to sample new data

points. Because of the latent manifold’s complex geometry, attempts using simple distributions (e.g., Gaussian) for the latent space have not provided satisfactory results.

Nonparametric vines naturally fill this gap. After training an autoencoder, we use its encoder component to extract lower dimensional feature representations of the data. Then, we fit a vine without additional restrictions on the latent distribution. With this simple step, we transform the autoencoders into generators, by systematically sampling data from the vine copula, following the procedure from Section 2.4. Finally, we use the decoder to transform the samples from vine in latent space into simulated images in pixel space. A schematic representation of this idea is given in Figure 1.

The vine copula is fitted post-hoc for two reasons. First, since the nonparametric estimator is consistent for (almost) any distribution, the only purpose of the AE is to minimize the reconstruction error. The AE’s latent space is unconstrained and the same AE can be used for both conditional and unconditional sampling. Second, it is unclear how to train a model that includes a nonparametric estimator since it has no parameters, there is no loss function to minimize or gradients to propagate. One possibility would be using spline estimators, which would allow to train the model end-to-end by fitting the basis expansion’s coefficients. However, spline estimators of copula densities have been empirically shown to have inferior performance than the transformation kernel estimator [52].

There is some leeway in modeling choices related to the vine. For instance, the number of trees as well as the choice of copula family (i.e., Gaussian or nonparametric) have an impact of the synthetic samples, as sharper details are expected from more flexible models. Note that one can adjust the characteristics of the vine until an acceptable fit of the latent features even after the autoencoder is trained.

4 Experiments

To evaluate vines as generative models, we follow a similar experimental setup as related works on GANs and VAEs. We compare vanilla VAEs to VCAEs using the same architectures, but replacing the variational part of the VAEs by vines to obtain the VCAEs. From the generative adversarial framework, we compare to DCGAN [58]. The architectures for all networks are described in the supplementary material.

Additionally, we explore two modifications of VCAE, (i) Conditional VCAE, that is sampling from a mixture obtained by fitting one vine per class label, and (ii) DEC-VCAE, namely adding a clustering-related penalty as in [74]. The rationale behind the clustering penalty was to better disentangle the features in the latent space. In other words, we obtain latent representations where the different clusters (i.e., classes) are better separated, thereby facilitating their modeling.

Metrics

To compare two distributions, it is common to estimate a density on the sampled data and then evaluate the log-likelihood of real test samples with the fitted density. However, it is known that the quality of sampled images cannot be simply measured by the log-likelihood [69]. Hence, we use the negative log-likelihood (NLL) and *coverage*², a closely related metric [71], only on two dimensional toy datasets in the supplementary material.

To quantitatively evaluate the image samples from vines, we use a recent evaluation framework for GANs [75]. According to [75], the most robust metrics for two sample testing are the *classifier two sample test* (C2ST, [44]) and *mean maximum discrepancy score* (MMD, [21]). Furthermore, [75] proposes to use these metrics not only in the pixel space, but over feature mappings in convolution space. Hence, we also compare generative models in terms of Wasserstein distance, MMD score and C2ST accuracy over ResNet-34 features. Additionally, we also use the *common inception score* [61] and *Fréchet inception distance* (FID, [26]). For all metrics, lower values are better, except for inception. We refer the reader to [75] for further details on the metrics and the implementation.

Experimental setup We use three real-world datasets: two small scale - MNIST [38] and Street View House Numbers [54], and one large scale - CelebA [42].

²Coverage measures the probability mass of the true data covered by the approximate density of the learned model as $C := P_{data}(dP_{model} > t)$. t is selected such that $P_{model}(dP_{model} > t) = \alpha$. We set $\alpha = 0.95$ as in the original paper.

For all models, we fix the autoencoder architecture, seeds and parameters of the optimizers as described in the supplementary material. Unless stated otherwise, all experiments were run with nonparametric vines and truncated after 5 trees. We use deep CNN models for the autoencoders in all baselines and follow closely DCGAN [58] with batch normalization layers for natural image datasets. For all autoencoder-based methods, we use Adam optimizer with learning rate 0.005 and weight decay 0.001 for all the natural image experiments, and 0.001 for both parameters on MNIST. For DCGAN we use the recommended learning rate 0.0002 and $\beta_1 = 0.5$ for Adam. The size of the latent spaces z was selected depending on the datasets's size and complexity. For MNIST, we present results with $z = 10$, SVHN $z = 20$ and for CelebA $z = 100$. We chose to present the values that gave reasonable results for all baselines. For MNIST, we used batch size of 128, for SVHN 32, and for CelebA batches of 100 samples for training. All models were trained on a separate train set, and evaluated on hold out test sets of 2000 samples, which is the evaluation size used in [75]. We used Pytorch 4.1 [55], and we provide our code in the supplementary material. All experiments were executed on an AWS instance *p2.xlarge* with an NVIDIA K80 GPU, 4 CPUs and 61 GB of RAM.

4.1 Image datasets

MNIST In Figure 4, we present results from VCAE to understand how different copula families impact the quality of the samples. The independence copula corresponds to assuming independence between the latent features as in VAEs. As in the toy datasets, nonparametrics seem to provide improvement over the other two. Within our framework, since the training of autoencoder and the vine fit are independent, we can use this to provide conditional sampling. We show results of vine samples per digit class in Figure 4.

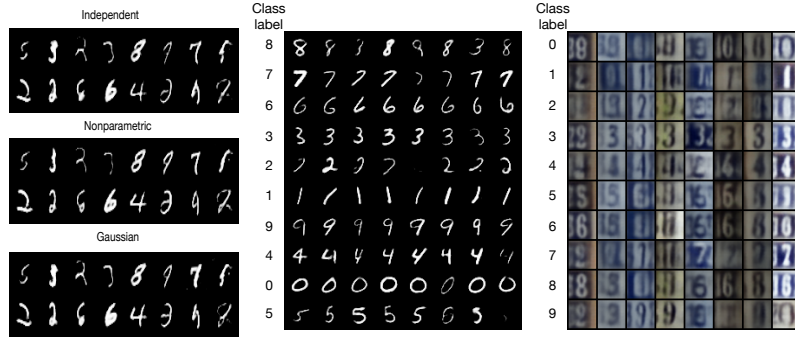


Figure 4: Left - impact of copula family selection in image sampling. Right - Random samples of Conditional VCAE on MNIST and SVHN

SVHN The results in Figure 5 show that the variants of vine generative models visually provide sharper images than vanilla VAEs when architectures and training hyper-parameters are the same for all models. All autoencoder-based methods were trained on latent space $z = 20$ for 200 epochs, while for DCGAN we use $z = 100$ and evaluate it at its best performance (50 epochs). In Figure 6, we can see that VCAE and DEC-VCAE have very similar and competitive results to DCGAN (at its best) across all metrics, and both clearly outperform vanilla VAE. Finally, the FID score calculated with regards to 10^4 real test samples are 0.205 for VAE, 0.194 for DCGAN and 0.167 for VCAE which shows that VCAE also has slight advantage using this metric.

CelebA

In the large scale setting, we present results for VCAE and VAE only, because our GPU ran out of memory on DEC-VCAE. From the random samples in Figure 7, we see that, for the same amount of training (in terms of epochs), VCAE results is not only sharper but also produce more diverse samples. VAEs improve using additional training, but vine-based solutions achieve better results with less resources and without constraints on the latent space.

To see the effect of the number of trees in the vine structure, we include Figure 8, where we can see that from the random sample the vine with five trees provides images with sharper details. Finally, as for SVHN, the FID score shows an advantage of the vine-base method over VAEs as we find 0.247 for VAE and 0.233 for VCAE. For DCGAN the FID score is



7 Figure 8: Higher truncation - sharper images.

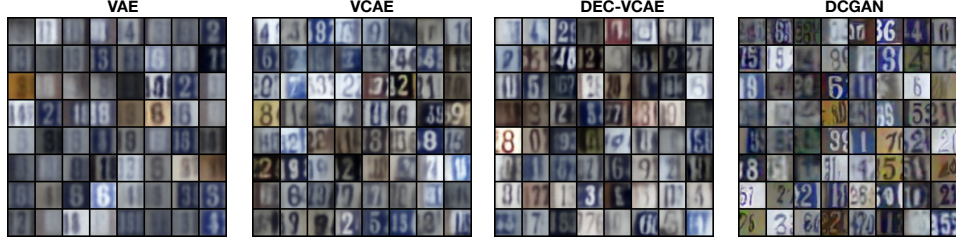


Figure 5: Left to right, random samples of VAE, VCAE, DEC-VCAE and DCGAN for SVHN.

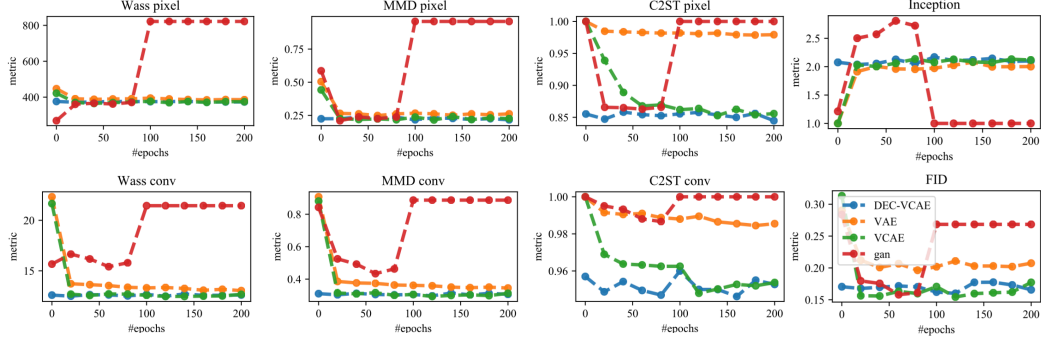


Figure 6: Various evaluation scores for all baselines on the SVHN dataset.

0.169 which is better than VCAE, however, looking at the random batch samples in Figure 7 although GANs outputs sharper images, it is clear that vine copula AE produces much more realistic faces.

Execution time We conclude the experimental section with Table 1. We note that VCAE has competitive execution times compared to VAE. Comparison to VAE instead of DCGAN is emphasized because VCAE and VAE have similar architectures and are closer framework-wise. Due to the different nature of these two frameworks (autoencoder and generative based) we cannot “fairly” compare in terms of execution time.

It should also be noted that the implementation of VCAE is far from optimal for two reasons. First, we use the R interface to vinecopulib in Python through rpy2. As such, there is a communication overhead resulting from switching between R and Python. Second, while vinecopulib uses multithreading, it is not parallelized to run on GPUs. From the results obtain, we do not think that this is problematic, since the execution times are satisfactory. But VCAE could be much faster if the Gaussian kernel estimators that we use were implemented within a tensor-based framework.

Table 1: Execution times.

	MNIST (200 eph)	SVHN (200 eph)	CelebA (100 eph)
VAE	50 min	4h 7 min	7h
VCAE	55 min	1h 32 min	6.5h
DEC VCAE	101 min	2h 35 min	/
DCGAN	120 min (40 epochs)	3h 20 min (50 epochs)	5h (30 epochs)

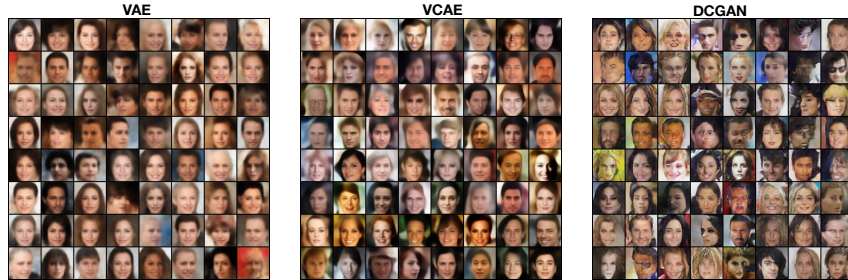


Figure 7: Random samples from left - VAE, - VCAE on CelebA, both trained for 200 epochs. - DCGAN best results at 30 epochs.

5 Conclusion

In this paper, we present vine copula autoencoders (VCAE), a first attempt at using copulas as high-dimensional generative models. VCAE leverage the capacities of autoencoders at providing compressed representations of the data, along with the flexibility of nonparametric vines to model arbitrary probability distributions. We highlight the versatility and power of vines as generative models in high-dimensional settings with results on various datasets. Several directions for future work and extensions are being considered. First, we started to experiments with VAEs having flexible distributional assumptions (i.e., by using a vine on the variational distribution). Second, we plan on studying hybrid models using adversarial mechanisms. There can also be extensions to text data, or investigating which types of vines synthesize best samples for different data types.

A Algorithm

A.1 Example of 5-dimensional vine copula

Example 1. The density of a PCC corresponding to the tree sequence in Figure 9 is

$$c = c_{1,2} c_{1,3} c_{3,4} c_{3,5} c_{2,3|1} c_{1,4|3} c_{1,5|3} c_{2,4|1,3} c_{4,5|1,3} c_{2,5|1,3,4}, \quad (3)$$

where the colors correspond to the edges E_1, E_2, E_3, E_4 .

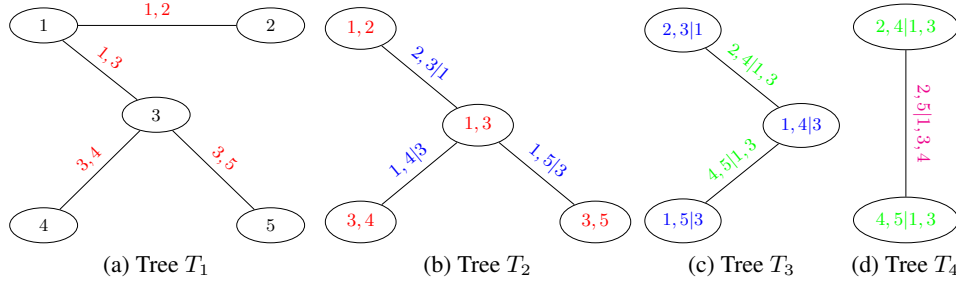


Figure 9: A vine tree sequence: the numbers represent the variables, x, y the bivariate distribution of x and y , and $x, y|z$ the bivariate distribution of x and y conditional on z . Each edge corresponds to a bivariate pair-copula in the PCC.

A.2 The VCAE algorithm

The algorithm for vine copula autoencoders is given in 1.

Algorithm 1 Vine Copula Autoencoder

Input: train set X of $\{x_1, x_2, \dots, x_n\}$ images.

1. Train autoencoder component with X :

$f \leftarrow \text{encoder}$

$g \leftarrow \text{decoder}$

2. Encode train set with f :

$\phi(X) \leftarrow f(X)$

3. Fit a vine copula c using encoded features:

$c \leftarrow \{\phi_1, \phi_2, \dots, \phi_n\}$ (as described in Sec 2.2 and 2.3).

4. Sample random observations from c :

$\phi' \leftarrow c(\phi)$ (as in Sec 2.4)

5. Decode the random features:

$X' \leftarrow g(\phi')$

Output: generated images X' .

Table 2: Evaluation on toy datasets for nonparametric and Gaussian copula. Average and standard deviations from 100 repetitions.

	Ring	Grid	Swiss roll
nonparametric			
NLL \uparrow	-2.47(0.15)	-3.77(0.2)	-5.23(0.05)
Coverage \uparrow	0.93(0.02)	0.94(0.02)	0.99(0.01)
MMD \downarrow	0.18(0.02)	0.15(0.16)	0.32(0.03)
Gaussian			
NLL \uparrow	-2.98(0.05)	-3.34(0.07)	-6.21(0.05)
Coverage \uparrow	0.95(0.02)	0.96(0.014)	0.93(0.03)
MMD \downarrow	0.33(0.02)	0.14(0.02)	0.38(0.02)

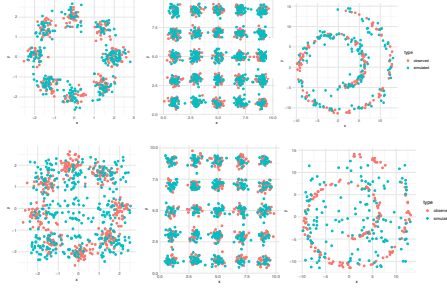


Figure 10: Copula generated data - top row nonparametric, bottom row Gaussian copula.

A.3 Variations of VCAE

Conditional VCAE Since the vine estimation and the AE training are independent in our approach, we can do steps 3–5 in 1 per class label (fit a vine per class feature) which makes the implementation of Conditional VCAE straightforward.

DEC-VCAE For the implementation of the DEC-VCAE we followed the instructions from the authors in [74]. A difficulty with autoencoders is that the encoded features are typically entangled, even when the AE reconstruction is accurate. Therefore we enforce some clustering. We start with an pre-trained AE and then optimize a two-term loss function: the clustering and the reconstruction loss.

B Toy datasets

Similarly to related generative model literature [24, 71], we test our method on two-dimensional toy datasets. Since this is a 2D case, we use bivariate copulas with nonparametric marginal densities for the estimation and sampling. The three datasets are ring of isotropic Gaussians with 8 modes, 5×5 grid of isotropic Gaussians and the swiss role dataset. These datasets have proven to be challenging for GANs due to the mode collapse issue [24, 71]. They motivate how the flexibility of nonparametric copulas can be leveraged, and we additionally compare to a baseline Gaussian copula. From Figure 10, we observe the benefits of using nonparametrics; while fitting such datasets is easy, it is clear that the Gaussian assumption is not suitable in such cases (except for the grid of Gaussians).

We further confirm this quantitatively in Table 2, where we repeat the experiment on 100 random datasets of each type, and present the average and standard deviations for both copula families. As expected, nonparametrics provide better samples according to the three two-sample metrics.

C Additional details on experiments

We use the same auto-encoder architecture for VCAE, DEC-VCAE and VAE as described below. All the autoencoders were trained by minimizing the Binary Cross Entropy Loss.

C.1 MNIST

The only transformation performed on this dataset is a padding of 2. By doing so we are able to use the same architecture for multiple datasets. We use CNNs for the encoder and the decoder whose architectures are as follows:

- Encoder:

$$\begin{aligned}
 x \in \mathbb{R}^{32 \times 32} &\rightarrow \text{Conv}_{32} \rightarrow \text{BN} \rightarrow \text{ReLU} \\
 &\rightarrow \text{Conv}_{64} \rightarrow \text{BN} \rightarrow \text{ReLU} \\
 &\rightarrow \text{Conv}_{128} \rightarrow \text{BN} \rightarrow \text{ReLU} \\
 &\rightarrow \text{FC}_{10}
 \end{aligned}$$

- Decoder:

$$\begin{aligned}
z \in R^{10} \rightarrow FC_{100} \rightarrow ConvT_{128} \rightarrow BN \rightarrow ReLU \\
\rightarrow ConvT_{64} \rightarrow BN \rightarrow ReLU \\
\rightarrow ConvT_{128} \rightarrow BN \rightarrow ReLU \\
\rightarrow FC_1
\end{aligned}$$

- DCGAN Generator:

$$\begin{aligned}
z \in R^{100} \rightarrow ConvT_1 \rightarrow BN \rightarrow ReLU \\
\rightarrow ConvT_{128} \rightarrow BN \rightarrow ReLU \\
\rightarrow ConvT_{64} \rightarrow BN \rightarrow ReLU \\
\rightarrow ConvT_{32} \rightarrow BN \rightarrow ReLU \\
\rightarrow ConvT_{16} \rightarrow BN \rightarrow ReLU \\
\rightarrow Tanh_1
\end{aligned}$$

- DCGAN Discriminator:

$$\begin{aligned}
Conv_1 \rightarrow BN \rightarrow LeakyReLU \\
\rightarrow Conv_{16} \rightarrow BN \rightarrow LeakyReLU \\
\rightarrow Conv_{32} \rightarrow BN \rightarrow LeakyReLU \\
\rightarrow Conv_{64} \rightarrow BN \rightarrow LeakyReLU \\
\rightarrow Conv_{128} \rightarrow BN \rightarrow LeakyReLU \\
\rightarrow Sigmoid_1
\end{aligned}$$

with all (de)convolutional layers have 4×4 filters, a stride of 2, and a padding of 1. We use BN to denote batch normalization and ReLU for rectified linear units and FC for fully connected layers. We denote $Conv_k$ the convolution with k filters. Leaky ReLU was used with negative slope = 0.2 everywhere.

C.2 SVHN

For SVHN we use the data as is without any preprocessing. The architectures are:

- Encoder:

$$\begin{aligned}
x \in R^{3 \times 32 \times 32} \rightarrow Conv_{64} \rightarrow BN \rightarrow LeakyReLU \\
\rightarrow Conv_{128} \rightarrow BN \rightarrow LeakyReLU \\
\rightarrow Conv_{256} \rightarrow BN \rightarrow LeakyReLU \\
\rightarrow FC_{100} \rightarrow FC_{20}
\end{aligned}$$

- Decoder:

$$\begin{aligned}
z \in R^{20} \rightarrow FC_{100} \rightarrow ConvT_{256} \rightarrow BN \rightarrow ReLU \\
\rightarrow ConvT_{128} \rightarrow BN \rightarrow ReLU \\
\rightarrow ConvT_{64} \rightarrow BN \rightarrow ReLU \\
\rightarrow ConvT_{32} \rightarrow BN \rightarrow ReLU \\
\rightarrow FC_1
\end{aligned}$$

- DCGAN Generator:

$$\begin{aligned}
z \in R^{100} \rightarrow ConvT_{256} \rightarrow BN \rightarrow ReLU \\
\rightarrow ConvT_{128} \rightarrow BN \rightarrow ReLU \\
\rightarrow ConvT_{64} \rightarrow BN \rightarrow ReLU \\
\rightarrow ConvT_{32} \rightarrow BN \rightarrow ReLU \\
\rightarrow ConvT_3 \rightarrow BN \rightarrow ReLU \\
\rightarrow Tanh_1
\end{aligned}$$

- DCGAN Discriminator:

$$\begin{aligned}
& Conv_3 \rightarrow BN \rightarrow LeakyReLU \\
& \rightarrow Conv_{32} \rightarrow BN \rightarrow LeakyReLU \\
& \rightarrow Conv_{64} \rightarrow BN \rightarrow LeakyReLU \\
& \rightarrow Conv_{128} \rightarrow BN \rightarrow LeakyReLU \\
& \rightarrow Conv_{256} \rightarrow BN \rightarrow LeakyReLU \\
& \rightarrow Sigmoid_1
\end{aligned}$$

where all (de)convolutional the layers have 4×4 filters, a stride of 2, and a padding of 1. The rest of the notations are the same as before.

C.3 CelebA

For CelebA we first took central crops of 140×140 and then resized to resolution 64×64 . Note that only Fig. 9 in the main text is not a result of this preprocessing. The architectures used are as follows:

- Encoder:

$$\begin{aligned}
x \in R^{3 \times 64 \times 64} & \rightarrow Conv_{64} \rightarrow BN \rightarrow LeakyReLU \\
& \rightarrow Conv_{128} \rightarrow BN \rightarrow LeakyReLU \\
& \rightarrow Conv_{256} \rightarrow BN \rightarrow LeakyReLU \\
& \rightarrow Conv_{512} \rightarrow BN \rightarrow LeakyReLU \\
& \rightarrow FC_{100} \rightarrow FC_{100}
\end{aligned}$$

- Decoder:

$$\begin{aligned}
z \in R^{100} & \rightarrow FC_{100} \rightarrow ConvT_{512} \rightarrow BN \rightarrow ReLU \\
& \rightarrow ConvT_{256} \rightarrow BN \rightarrow ReLU \\
& \rightarrow ConvT_{128} \rightarrow BN \rightarrow ReLU \\
& \rightarrow ConvT_{64} \rightarrow BN \rightarrow ReLU \\
& \rightarrow ConvT_{32} \rightarrow BN \rightarrow ReLU \\
& \rightarrow FC_1
\end{aligned}$$

- DCGAN Generator:

$$\begin{aligned}
z \in R^{100} & \rightarrow ConvT_{512} \rightarrow BN \rightarrow ReLU \\
& \rightarrow ConvT_{256} \rightarrow BN \rightarrow ReLU \\
& \rightarrow ConvT_{128} \rightarrow BN \rightarrow ReLU \\
& \rightarrow ConvT_{64} \rightarrow BN \rightarrow ReLU \\
& \rightarrow ConvT_3 \rightarrow BN \rightarrow ReLU \\
& \rightarrow Tanh_1
\end{aligned}$$

- DCGAN Discriminator:

$$\begin{aligned}
& Conv_3 \rightarrow BN \rightarrow LeakyReLU \\
& \rightarrow Conv_{64} \rightarrow BN \rightarrow LeakyReLU \\
& \rightarrow Conv_{128} \rightarrow BN \rightarrow LeakyReLU \\
& \rightarrow Conv_{256} \rightarrow BN \rightarrow LeakyReLU \\
& \rightarrow Conv_{512} \rightarrow BN \rightarrow LeakyReLU \\
& \rightarrow Sigmoid_1
\end{aligned}$$

where all the (de)convolutional layers have 4×4 filters, a stride of 2, and a padding of 1. Padding was set to 0 only for the last convolutional layer of the encoder and the first layer of the decoder. The rest of the notations are the same as before.

D Interpolation in latent space

Next we include 11 which shows that, when walking the latent space by linear interpolation between two test samples as in [58], the transitions for VCAE are smooth and without any sharp changes or

unexpected samples in-between. This is not explicitly related to VCAE generative models since we do not train an end-to-end model, however it is important to show that the AE network we use did not simply memorize images.

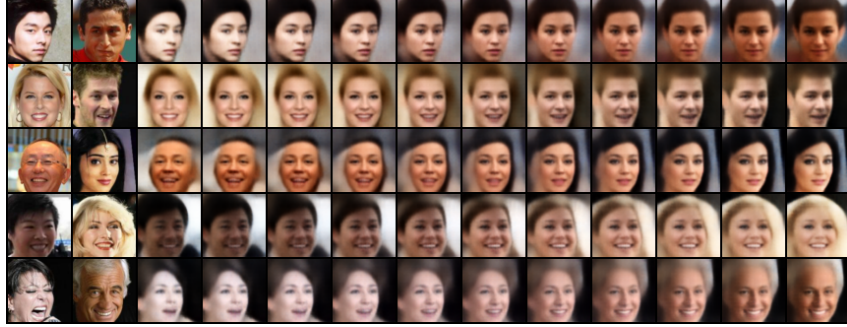


Figure 11: Interpolation in latent space between two real samples (shown in the first two columns) on **CelebA** using *VCAE*

E Simulating Mobility Trajectories with copulas

In related work [36], we have also compared to adversarial and recurrent based methods for *sampling sequential data* (artificial mobility trajectories). We evaluate the generated trajectories with respect to their geographic and semantic similarity, circadian rhythms, long-range dependencies, training and generation time. We also include two sample tests to assess statistical similarity between the observed and simulated distributions, and we analyze the privacy trade-offs with respect to membership inference and location-sequence attacks. The results show that copulas surpass all baselines in terms of MMD score and training + simulation time. For more details please see [36].

F Code

Our code is available at the following link: <https://github.com/tagas/vcae>.

References

- [1] K. Aas, C. Czado, A. Frigessi, and H. Bakken. Pair-Copula Constructions of Multiple Dependence. *Insurance: Mathematics and Economics*, 44(2):182–198, 2009.
- [2] Kjersti Aas. Pair-copula constructions for financial applications: A review. *Econometrics*, 4(4):43, October 2016. ISSN 2225-1146. doi: 10.3390/econometrics4040043. URL <http://www.mdpi.com/2225-1146/4/4/43/htm>.
- [3] Tim Bedford and Roger M. Cooke. Probability Density Decomposition for Conditionally Dependent Random Variables Modeled by Vines. *Annals of Mathematics and Artificial Intelligence*, 32(1-4):245–268, 2001.
- [4] Tim Bedford and Roger M. Cooke. Vines – A New Graphical Model for Dependent Random Variables. *The Annals of Statistics*, 30(4):1031–1068, 2002. doi: 10.1214/aos/1031689016.
- [5] Yoshua Bengio, Aaron Courville, and Pascal Vincent. Representation learning: A review and new perspectives. *IEEE transactions on pattern analysis and machine intelligence*, 35(8):1798–1828, 2013.
- [6] Hervé Bouchard and Yves Kamp. Auto-association by multilayer perceptrons and singular value decomposition. *Biological cybernetics*, 59(4-5):291–294, 1988.
- [7] Eike C. Brechmann and Harry Joe. Parsimonious parameterization of correlation matrices using truncated vines and factor analysis. *Computational Statistics and Data Analysis*, 77:233–251, 2014. ISSN 01679473. doi: 10.1016/j.csda.2014.03.002.
- [8] Eike Christian Brechmann and Claudia Czado. COPAR—multivariate time series modeling using the copula autoregressive model. *Applied Stochastic Models in Business and Industry*, 31(4):495–514, 2015. ISSN 1526-4025.
- [9] Eike Christian Brechmann and Harry Joe. Truncation of vine copulas using fit indices. *Journal of Multivariate Analysis*, 138:19–33, 2015. ISSN 0047-259X.
- [10] Eike Christian Brechmann and Ulf Schepsmeier. Modeling dependence with C-and D-vine copulas: The R-package CDVine. *Journal of Statistical Software*, 52(3):1–27, 2013.
- [11] Eike Christian Brechmann, Claudia Czado, and Kjersti Aas. Truncated regular vines in high dimensions with application to financial data. *Canadian Journal of Statistics*, 40(1):68–85, March 2012. ISSN 03195724. doi: 10.1002/cjs.10141.
- [12] Yale Chang, Yi Li, Adam Ding, and Jennifer Dy. A robust-equitable copula dependence measure for feature selection. *AISTATS*, 41:84–92, 2016.
- [13] Xi Chen, Yan Duan, Rein Houthooft, John Schulman, Ilya Sutskever, and Pieter Abbeel. Infogan: Interpretable representation learning by information maximizing generative adversarial nets. In *Advances in neural information processing systems*, pages 2172–2180, 2016.
- [14] Claudia Czado. Pair-Copula Constructions of Multivariate Copulas. In Piotr Jaworski, Fabrizio Durante, Wolfgang Karl Härdle, and Tomasz Rychlik, editors, *Copula Theory and Its Applications*, Lecture Notes in Statistics, pages 93–109. Springer Berlin Heidelberg, 2010.
- [15] Claudia Czado, Ulf Schepsmeier, and Aleksey Min. Maximum likelihood estimation of mixed C-vines with application to exchange rates. *Statistical Modelling*, 12(3):229–255, 2012. ISSN 1471-082X.
- [16] Claudia Czado, Eike Christian Brechmann, and Lutz Gruber. Selection of Vine Copulas. In Piotr Jaworski, Fabrizio Durante, and Wolfgang Karl Härdle, editors, *Copulae in Mathematical and Quantitative Finance: Proceedings of the Workshop Held in Cracow, 10-11 July 2012*, volume 36. Springer New-York, 2013.
- [17] J. Dissmann, Eike Christian Brechmann, Claudia Czado, Dorota Kurowicka, J. Dißmann, Eike Christian Brechmann, Claudia Czado, and Dorota Kurowicka. Selecting and estimating regular vine copulae and application to financial returns. *Computational Statistics & Data Analysis*, 59:52–69, March 2013. ISSN 01679473. doi: 10.1016/j.csda.2012.08.010. URL <http://www.sciencedirect.com/science/article/pii/S0167947312003131>.

- [18] Gal Elidan. Copulas in machine learning. In *Copulae in mathematical and quantitative finance*, pages 39–60. Springer, 2013.
- [19] Gery Geenens, Arthur Charpentier, and Davy Paindaveine. Probit transformation for nonparametric kernel estimation of the copula density. *Bernoulli*, 23(3):1848–1873, 2017.
- [20] Ian Goodfellow, Jean Pouget-Abadie, Mehdi Mirza, Bing Xu, David Warde-Farley, Sherjil Ozair, Aaron Courville, and Yoshua Bengio. Generative adversarial nets. In *Advances in neural information processing systems*, pages 2672–2680, 2014.
- [21] Arthur Gretton, Karsten M Borgwardt, Malte Rasch, Bernhard Schölkopf, and Alex J Smola. A kernel method for the two-sample-problem. In *Advances in neural information processing systems*, pages 513–520, 2007.
- [22] Paulina Grnarova, Kfir Y Levy, Aurelien Lucchi, Nathanael Perraudin, Thomas Hofmann, and Andreas Krause. Evaluating gans via duality. *arXiv preprint arXiv:1811.05512*, 2018.
- [23] Gaël Guennebaud, Benoît Jacob, and Others. Eigen v3, 2010. URL <http://eigen.tuxfamily.org>.
- [24] Ishaan Gulrajani, Faruk Ahmed, Martin Arjovsky, Vincent Dumoulin, and Aaron C Courville. Improved training of wasserstein gans. In *Advances in Neural Information Processing Systems*, pages 5767–5777, 2017.
- [25] Ingrid Hobæk Haff. Parameter estimation for pair-copula constructions. *Bernoulli*, 19(2): 462–491, 2013. ISSN 1350-7265.
- [26] Martin Heusel, Hubert Ramsauer, Thomas Unterthiner, Bernhard Nessler, Günter Klambauer, and Sepp Hochreiter. Gans trained by a two time-scale update rule converge to a nash equilibrium. *arXiv preprint arXiv:1706.08500*, 1(2):4, 2017.
- [27] Irina Higgins, Loic Matthey, Arka Pal, Christopher Burgess, Xavier Glorot, Matthew Botvinick, Shakir Mohamed, and Alexander Lerchner. beta-vae: Learning basic visual concepts with a constrained variational framework. 2016.
- [28] Geoffrey E Hinton and Ruslan R Salakhutdinov. Reducing the dimensionality of data with neural networks. *science*, 313(5786):504–507, 2006.
- [29] Geoffrey E Hinton and Richard S Zemel. Autoencoders, minimum description length and helmholtz free energy. In *Advances in neural information processing systems*, pages 3–10, 1994.
- [30] Geoffrey E Hinton, Simon Osindero, and Yee-Whye Teh. A fast learning algorithm for deep belief nets. *Neural computation*, 18(7):1527–1554, 2006.
- [31] Aapo Hyvärinen and Erkki Oja. Independent component analysis: algorithms and applications. *Neural networks*, 13(4-5):411–430, 2000.
- [32] Harry Joe. *Multivariate Models and Dependence Concepts*. Chapman & Hall/CRC, 1997.
- [33] Harry Joe. *Dependence modeling with copulas*. Chapman and Hall/CRC, 2014.
- [34] Matthias Killiches, Daniel Kraus, and Claudia Czado. Model distances for vine copulas in high dimensions. *Statistics and Computing*, pages 1–19, 2017. ISSN 0960-3174.
- [35] Diederik P Kingma and Max Welling. Auto-encoding variational bayes. *arXiv preprint arXiv:1312.6114*, 2013.
- [36] Vaibhav Kulkarni, Natasa Tagasovska, Thibault Vatter, and Benoit Garbinato. Generative models for simulating mobility trajectories. 2018.
- [37] Dorota Kurowicka and Harry Joe. *Dependence Modeling*. World Scientific Publishing Company, Incorporated, 2010. ISBN 978-981-4299-87-9. doi: 10.1142/7699.

- [38] Yann LeCun and Corinna Cortes. MNIST handwritten digit database. 2010. URL <http://yann.lecun.com/exdb/mnist/>.
- [39] Yann LeCun, Yoshua Bengio, et al. Convolutional networks for images, speech, and time series. *The handbook of brain theory and neural networks*, 3361(10):1995, 1995.
- [40] Haoran Li, Li Xiong, and Xiaoqian Jiang. Differentially Private Synthesization of Multi-Dimensional Data using Copula Functions. In *Proc. of the 17th International Conference on Extending Database Technology*, number c, pages 475–486, 2014. ISBN 9783893180653. doi: 10.5441/002/edbt.2014.43. URL <http://citeseerx.ist.psu.edu/viewdoc/download?doi=10.1.1.1.679.1970{%&}rep=rep1{%&}type=pdf>.
- [41] Han Liu, John Lafferty, and Larry Wasserman. The Nonparanormal: semiparametric estimation of high dimensional undirected graphs. *Journal of Machine Learning Research*, 10:2295–2328, 2009.
- [42] Ziwei Liu, Ping Luo, Xiaogang Wang, and Xiaoou Tang. Deep learning face attributes in the wild. In *Proceedings of International Conference on Computer Vision (ICCV)*, 2015.
- [43] David Lopez-Paz. *From Dependence to Causation*. PhD thesis, University of Cambridge, 2016.
- [44] David Lopez-Paz and Maxime Oquab. Revisiting classifier two-sample tests. *arXiv preprint arXiv:1610.06545*, 2016.
- [45] David Lopez-Paz, J M Hernandez-Lobato, and Bernhard Schölkopf. Semi-supervised domain adaptation with copulas. *NIPS* 26, pages 674–682, 2013.
- [46] Alireza Makhzani, Jonathon Shlens, Navdeep Jaitly, Ian Goodfellow, and Brendan Frey. Adversarial autoencoders. *arXiv preprint arXiv:1511.05644*, 2015.
- [47] Luke Metz, Ben Poole, David Pfau, and Jascha Sohl-Dickstein. Unrolled generative adversarial networks. *ICLR*, 2016.
- [48] Thomas Nagler and Claudia Czado. Evading the curse of dimensionality in nonparametric density estimation with simplified vine copulas. *Journal of Multivariate Analysis*, 151:69–89, 2016. ISSN 0047259X. doi: 10.4171/OWR/2015/20. URL <http://arxiv.org/abs/1503.03305>.
- [49] Thomas Nagler and Thibault Vatter. vinecopulib: High Performance Algorithms for Vine Copula Modeling in C++. <http://vinecopulib.org>, 2017.
- [50] Thomas Nagler and Thibault Vatter. *kde1d: Univariate Kernel Density Estimation*, 2018. URL <https://CRAN.R-project.org/package=kde1d>. R package version 0.2.1.
- [51] Thomas Nagler and Thibault Vatter. rvinecopulib: high performance algorithms for vine copula modeling, 2018. URL <https://cran.r-project.org/package=rvinecopulib>.
- [52] Thomas Nagler, Christian Schellhase, and Claudia Czado. Nonparametric estimation of simplified vine copula models: comparison of methods. *Dependence Modeling*, 5(1):99–120, 2017.
- [53] Roger B Nelsen. *An introduction to copulas*. Springer Science & Business Media, 2007.
- [54] Yuval Netzer, Tao Wang, Adam Coates, Alessandro Bissacco, Bo Wu, and Andrew Y Ng. Reading digits in natural images with unsupervised feature learning. In *NIPS workshop on deep learning and unsupervised feature learning*, volume 2011, page 5, 2011.
- [55] Adam Paszke, Sam Gross, Soumith Chintala, Gregory Chanan, Edward Yang, Zachary DeVito, Zeming Lin, Alban Desmaison, Luca Antiga, and Adam Lerer. Automatic differentiation in pytorch. 2017.
- [56] Neha Patki, Roy Wedge, and Kalyan Veeramachaneni. The synthetic data vault. *Proceedings - 3rd IEEE International Conference on Data Science and Advanced Analytics, DSAA 2016*, pages 399–410, 2016. doi: 10.1109/DSAA.2016.49. URL <https://dai.lids.mit.edu/wp-content/uploads/2018/03/SDV.pdf>.

- [57] R Core Team. R: A language and environment for statistical computing, 2017. URL <https://www.r-project.org/>.
- [58] Alec Radford, Luke Metz, and Soumith Chintala. Unsupervised representation learning with deep convolutional generative adversarial networks. *arXiv preprint arXiv:1511.06434*, 2015.
- [59] Danilo Jimenez Rezende and Shakir Mohamed. Variational inference with normalizing flows. *arXiv preprint arXiv:1505.05770*, 2015.
- [60] Murray Rosenblatt. Remarks on a multivariate transformation. *The annals of mathematical statistics*, 23(3):470–472, 1952.
- [61] Tim Salimans, Ian Goodfellow, Wojciech Zaremba, Vicki Cheung, Alec Radford, and Xi Chen. Improved techniques for training gans. In *Advances in Neural Information Processing Systems*, pages 2234–2242, 2016.
- [62] Olivier Scaillet, Arthur Charpentier, and Jean-David Fermanian. The estimation of copulas: Theory and practice. Technical report, Ensaie-Crest and Katholieke Universiteit Leuven, NP-Paribas and Crest; HEC Geneve and Swiss Finance Institute, 2007.
- [63] Boris Schöling. *The Boost C++ Libraries*. 2011.
- [64] Ulf Schepsmeier and Jakob Stöber. Derivatives and Fisher information of bivariate copulas. *Statistical Papers*, 55(2):525–542, May 2014. ISSN 0932-5026. doi: 10.1007/s00362-013-0498-x.
- [65] Simon J Sheather and Michael C Jones. A reliable data-based bandwidth selection method for kernel density estimation. *Journal of the Royal Statistical Society. Series B (Methodological)*, pages 683–690, 1991.
- [66] A. Sklar. Fonctions de Répartition à n Dimensions et Leurs Marges. *Publications de L’Institut de Statistique de L’Université de Paris*, 8:229–231, 1959.
- [67] Jakob Stöber and Claudia Czado. Sampling Pair Copula Constructions with Applications to Mathematical Finance. In Jan-Frederik Mai and Matthias Scherer, editors, *Simulating Copulas: Stochastic Models, Sampling Algorithms and Applications*, Series in quantitative finance. World Scientific Publishing Company, Incorporated, 2012.
- [68] Jakob Stöber and Ulf Schepsmeier. Estimating standard errors in regular vine copula models. *Computational Statistics*, 28(6):2679–2707, 2013. ISSN 0943-4062.
- [69] Lucas Theis, Aäron van den Oord, and Matthias Bethge. A note on the evaluation of generative models. In *ICLR*, 2015. ISBN 1511.01844. doi: 10.1177/096032717100300408. URL <http://arxiv.org/abs/1511.01844>.
- [70] Ilya Tolstikhin, Olivier Bousquet, Sylvain Gelly, and Bernhard Schoelkopf. Wasserstein auto-encoders. *arXiv preprint arXiv:1711.01558*, 2017.
- [71] Ilya O Tolstikhin, Sylvain Gelly, Olivier Bousquet, Carl-Johann Simon-Gabriel, and Bernhard Schölkopf. Adagan: Boosting generative models. In *Advances in Neural Information Processing Systems*, pages 5424–5433, 2017.
- [72] Dustin Tran, David M Blei, and Edoardo M Airoldi. Copula variational inference. In *NIPS* 28, pages 3564–3572, 2015.
- [73] Pascal Vincent, Hugo Larochelle, Yoshua Bengio, and Pierre-Antoine Manzagol. Extracting and composing robust features with denoising autoencoders. In *Proceedings of the 25th international conference on Machine learning*, pages 1096–1103. ACM, 2008.
- [74] Junyuan Xie, Ross Girshick, and Ali Farhadi. Unsupervised deep embedding for clustering analysis. In *International conference on machine learning*, pages 478–487, 2016.
- [75] Qiantong Xu, Gao Huang, Yang Yuan, Chuan Guo, Yu Sun, Felix Wu, and Kilian Weinberger. An empirical study on evaluation metrics of generative adversarial networks. *arXiv preprint arXiv:1806.07755*, 2018.